Activation of persulfate by homogeneous and heterogeneous iron catalyst to degrade chlortetracycline in aqueous solution

Rama Pulicharla[a], Roggy Drouinaud[b], Satinder Kaur Brar[a]*, Patrick Drogui[a], Francois Proulx[b], Mausam Verma[c], Rao Y. Surampalli[d]

[a] INRS-ETE, Université du Québec, 490, Rue de la Couronne, Québec, Canada G1K 9A9.

[b] Service du traitement des eaux, 214, Avenue St-Sacrement, suite 210, Québec, Canada G1N 3X6.

[c] CO2 Solutions Inc., 2300, Rue Jean-Perrin, Québec, Québec G2C 1T9 Canada.

[d] Department of Civil Engineering, University of Nebraska-Lincoln, N104 SEC PO Box 886105, Lincoln, NE 68588-6105, USA.

[a]* Corresponding author: INRS-ETE, Université du Québec, 490, Rue de la Couronne, Québec, Canada G1K 9A9. E-mail: satinder.brar@ete.inrs.ca; Téléphone: + 418 654 3116; Fax: + 418 654 2600.

Abstract:

This study investigates the removal of chlortetracycline (CTC) antibiotic using sulfate radical-based oxidation process. Sodium persulfate (PS) was used as a source to generate sulfate radicals by homogeneous (Fe^{2+}) and heterogeneous (zero valent iron, ZVI) iron as a catalyst. Increased EDTA concentration was used to break the CTC-Fe metal complexes during CTC estimation. The influence of various parameters, such as PS concentration, iron (Fe^{2+} and ZVI) concentration, PS/iron molar ratio, and pH were studied and optimum conditions were reported. CTC removal was increased with increasing concentration of PS and iron at an equal molar ratio of PS/Fe^{2+} and PS/ZVI processes. PS/Fe^{2+} and PS/ZVI oxidation processes at 1:2 (500 µM PS and 1000 µM) molar ratio showed 76% and 94% of 1 µM CTC removal in 2h. Furtherincreased molar ratio 1:2

onwards, PS/Fe^{2+} process showed a slight increase in CTC degradation whereas in PS/ZVI process showed similar degradation to 1:2 (PS/Fe) ratio at constant PS 500 µM concentration. Slower activation of persulfate which indirectly indicates the slower generation of sulfate radicals in PS/ZVI process showed higher degradation efficiency of CTC. The detected transformation products and their estrogenicity results stated that sulfate radicals seem to be efficient in forming stable and non-toxic end products.

Keywords: chlortetracycline, iron, metal complexation, sulfate radicals, homogeneous catalyst, heterogeneous catalyst.

Highlights:

Higher EDTA concentration was used to break CTC-Fe complexes

Low ZVI dose and slow activation of persulfate resulted in efficient degradation

Dechlorinated end products were seen by sulfate radical degradation

No estrogenic effects were observed for the treated CTC solution

Introduction

Continuous detection of contaminants in water sources demands their efficient removal. Currently, advanced oxidation processes (AOPs) have been competently used in the removal of emerging contaminants in wastewater. AOPs such as ozonation (Michael-Kordatou et al., 2017), Fenton (Munoz et al., 2016), ultrasonic (Mecha et al., 2016), photo-Fenton (Miralles-Cuevas et al., 2014), photocatalytic (Paul et al., 2007; Qin et al., 2016), and persulfate (Anipsitakis and Dionysiou; Lin et al., 2016) oxidation processes have proven to be efficient in degrading recalcitrant emerging pollutants. Continuous and trace detection of pollutants demands technological advances in AOPs

to meet current environmental regulations. Almost all AOPs involves generation of hydroxyl radicals ($OH^{\bullet}$) which are non-selective towards most of the organic contaminants (Lee and von Gunten, 2010). The oxidants used for the generation of $OH^{\bullet}$, such as ozone, hydrogen peroxide, and permanganate have selective reactivity towards unsaturated compounds such as fatty esters, unsaturated alcohols, etc. This property makes these oxidants inefficient in the complete mineralization of recalcitrant contaminants having complex structure due to their selective oxidation (Gogate and Pandit, 2004).

PS oxidant has recently drawn much attention from researchers to overcome these limitations of oxidants producing $OH^{\bullet}$. PS has higher solubility and stability at room temperature and has high oxidation potential (E^0 = 2.01 V) (Liang et al., 2004; Zhou et al., 2013). And activation of PS produces high redox potential and non-selective sulfate radical (SO_4^{-*}, E^0 = 2.6 V) similar to $OH^{\bullet}$ (Vicente et al., 2011). Moreover, SO_4^{-*} induces hydroxyl radical's generation as per Eq. 3. Generation of $OH^{\bullet}$ along with sulfate radicals having similar oxidation potential might increase the efficacy of the system to degrade the contaminants.

Different approaches have been used to activate PS, such as increasing temperature (Luo, 2014), addition of transition metal ions (Anipsitakis and Dionysiou, 2004) or chelation agents (Liang et al., 2009), or by ultraviolet irradiation (UV) (Lau et al., 2007). Among these, iron (Fe) based metal activation was most studied and reported for efficient SO_4^{-*} production (Oh et al., 2009; Monteagudo et al., 2015). Moreover, an iron-based catalyst has both homogeneous (Fe^{2+}; soluble) and heterogeneous (Fe^0, insoluble) ways to activate persulfate (Gao et al., 2016). Cost-effectiveness, natural presence, and high activity of iron making it as a promising catalyst to

activate the PS and generat sulfate radicals (Liang et al., 2004; Romero et al., 2010). Overall reactions involved in the process of generating SO_4^{-*} by activation of PS by ZVI and Fe^{2+} are described by Eq. 1-7 (Wilmarth et al., 1962; McElroy and Waygood, 1990; Liang et al., 2007; Triszcz et al., 2009).

$$S_2O_8^{2-} + Fe^{2+} \rightarrow Fe^{3+} + SO_4^{-*} \quad (1)$$

$$S_2O_8^{2-} + Fe^{2+} \rightarrow Fe^{3+} + SO_4^{2-} + SO_4^{-*} \quad (2)$$

$$SO_4^{-*} + H_2O \rightarrow OH^* + H^+ + SO_4^{2-} \quad (3)$$

$$SO_4^{-*} + Fe^{2+} \rightarrow Fe^{3+} + SO_4^{2-} \quad (4)$$

$$SO_4^{*-} + SO_4^{-*} \rightarrow 2SO_4^{2-} \quad (5)$$

$$SO_4^{-*} + OH^* \rightarrow HSO_4^- \quad (6)$$

$$S_2O_8^{2-} + Fe^0 \rightarrow Fe^{2+} + SO_4^{2-} \quad (7)$$

$$Fe^{3+} + Fe^0 \rightarrow Fe^{2+} \quad (8)$$

$$Fe^0 + H_2O \rightarrow Fe^{2+} + H_2 + OH^- \quad (9)$$

Tetracycline antibiotics are largely used in humans, veterinary, and aquaculture applications either for diseases prevention or for growth promotion due to their broad-spectrum activity. Researchers reported the omnipresence of tetracyclines around 0.11−48 μg/L (Miao et al., 2004; Karthikeyan and Meyer, 2006; Puicharla et al., 2014) in water and wastewater sources. Chlortetracycline (CTC) is the first tetracycline antibiotichas a four-ring system with multiple O- and N-containing ionizable functional groups which form strong complexes with metals including iron (Pulicharla et al., 2015; Wang et al., 2015). Fig. 1 shows the binding site of Fe^{2+} metal in CTC structure. CTC-

Fe complex affects CTC redox reactions by decreasing the availability of lone pair electrons (-OH and $–NH_2$) which are susceptible to oxidative reactions. Until date, many oxidation technologies were developed to degrade CTC in the aqueous solution such as ozonation, UV and photocatalysis treatments and were efficient to remove 90% of CTC (Daghrir et al., 2012; Guo and Chen, 2012; Kim et al., 2012; Daghrir et al., 2013; Hammad Khan et al., 2013). However, to our knowledge, PS/Fe^{2+} (homogeneous) and PS/ZVI (heterogeneous) processes have never been attempted to degrade CTC. According to studies, SO_4^{-*} can be rapidly scavenged by excess Fe^{2+} in the case of PS/Fe^{2+} process (Eq. 4), which decrease the pollutant degradation efficiency (Liang et al., 2004). Use of ZVI powder alternative to Fe^{2+} has been reported in the literature to overcome this disadvantage (Liang and Guo, 2010; Deng et al., 2014). Further, ZVI is able to produce and regenerate Fe^{2+} by reduction of PS (Eq. 7) and Fe^{3+} (Eq. 8), respectively. Even though persulfate ($S_2O_8^{2-}$) transforms into an undesired product (SO_4^{2-}) (Eq. 7), still Fe^0 generation from Fe^{2+} is necessary to activate persulfate to produce sulfate radicals.

The scope of this study is to evaluate the degradation efficiency of CTC by PS/Fe^{2+} and PS/ZVI processes; specifically focuses on 1) method development to estimate the free CTC after complexation with iron using ultra high-pressure liquid chromatography-mass spectrometry (UHPLC-MS/MS); 2) PS/Fe^{2+} and PS/ZVI ratio optimization to produce sulfate radicals by PS activation to degrade CTC; 3) comparison of degradation efficiencies of CTC by PS/Fe^{2+} and PS/ZVI processes; 4) identification of degradation products and pathways; and 5) toxicity measurement of degraded CTC by determining estrogenicity. Estrogenicity is defined as the effect of CTC and its by-products on the fauna to develop female secondary sex characteristics, growth, and maturation of long bones.

2. Material and methods

2.1 Chemicals

CTC with 99% purity was purchased from Toronto Research Chemicals (Toronto, Canada). Disodium ethylenediaminetetraacetate (Na_2H_2EDTA, 99%) was purchased from E-bay (Tokyo, Japan). Methanol (HPLC grade, purity >99.8%), acetonitrile (ACN, UHPLC grade, purity >99.9%), formic acid (UHPLC grade, purity >99.9%) were purchased from Fisher Scientific (Ontario, Canada). Sodium persulfate (>98%), sodium azide (>99.9%), 1, 10-phenanthroline (>99%), 5-sulfosalicylic acid hydrate (>95%), potassium iodide (99%) and sodium bicarbonate, were obtained from Sigma-Aldrich (St. Louis, USA). Iron powder was purchased from Fisher scientific (Nazareth, USA). The particle size of the iron powder was found to be 0.4-1mm determined using Laser Horiba particle size 133 analyzer (LA-950, NJ, USA) and reported density was 7.86 g/L. Milli-Q/Reference with an LC-PAK polisher cartridge installed at the point-of-use and Milli-Q/Milli-RO Millipore systems (Milford, MA, USA) were used to prepare UHPLC and HPLC grade water in the laboratory.

2.2 Experimental procedure

Initial CTC degradation experiments were conducted for optimization of PS/Fe^{2+} and PS/ZVI processes. All the experiments were performed in 250 mL glass flasks with a total solution volume of 100 mL at 20±2 ^{o}C. PS/Fe^{2+} degradation experiments were carried out under constant stirring with a magnetic stirrer at 500 rpm and for PS/ZVI process, homogenizer at 500 rpm was used to mix PS and ZVI for 2h. Concentrations of PS were taken based on the proposed stoichiometric Eq. 10. For PS optimization, a ratio of 1:1 (PS: iron) was taken with five different concentrations including 100, 250, 500, 1000, 5000 µM by keeping constant CTC concentration of 1 µM (0.479

mg/L) for both PS/Fe^{2+} and PS/ZVI processes, CTC concentrations ranging from 0.1–0.6 µg/L in wastewater effluent (Karthikeyan and Meyer, 2006), surface water (Lindsey et al., 2001) , 0.19-3.8 mg/kg in sludge, 0.08-1.5 mg/kg in soil and 0.1-139 mg/kg (An et al., 2015) in animal manure have been reported. The used CTC concentration in this study was selected within the range of detected CTC concentrations in different environmental samples. Once the PS concentration was optimized based on the CTC removal efficiency, optimal PS to Fe^{2+} or ZVI ratio was investigated under various PS to Fe^{2+} or Fe^{0} molar ratios, including 1:0.5, 1:1, 1:2, 1:3, and 1:4. After the optimization of PS/Fe^{2+} and PS/ZVI process ratios, pH effect ranging from 3-10 was studied. In all experiments, SO_4^{-*} generation was quenched with sodium nitrite 0.1 M and samples were filtered and stored at 4 ^{o}C, until CTC analysis. All experiments were carried out in triplicate and mean values of data was taken to present in all figures.

$$C_{22}H_{23}ClN_2O_8 + 48N_2S_2O_8 + 36H_2O \rightarrow 22CO_2 + 48Na_2SO_4 + 48H_2SO_4 + HCl + N_2 \qquad 10$$

2.3 Analytical methods

2.3.1 CTC estimation

2.3.1.1 Sample preparation for CTC analysis

All samples including standards and CTC experiments before and after degradation were filtered through acetone washed 2 mm glass fiber (Fisher brand G6 filter circles, Fisher Scientific, Ontario Canada). Sample preparation for CTC analysis followed the method of (Puicharla et al., 2014) with small modifications. EDTA concentration was optimized in this study to break the CTC-Fe complexes and get maximum CTC recovery. To 5 mL of CTC filtrate, EDTA of 1-10 mM was added before adjusting the pH with 5 N HCl to 2.7–3. After pH adjustment, samples were immediately subjected to clean-up with Sep-pack® C18 Plus Short Cartridges as mentioned in

(Puicharla et al., 2014). The final CTC extraction was stored at 4 ^{o}C until injecting into UHPLC. Loss of CTC during extraction was determined by spiking CTC in milli-Q water and for the matrix effects (Fe^{2+}, ZVI, and PS) determination, CTC was spiked in 5 mL milli-Q water containing respective matrix before extraction. The CTC was measured in UHPLC–MS/MS method developed in this study and spike recoveries were calculated by following Eq. 11

$$\% \, recovery = (C_f / C_i) \times 100 \qquad 11$$

where C_f = measured concentration of CTC after extraction, C_i = initial concentration of CTC spiked in the sample. Recoveries of spiked CTC were found to be 93–105%. This indicates the complete release of CTC from its iron metal complex with the developed method.

2.3.1.2 UHPLC–MS/MS

CTC was analyzed in the extraction samples by Waters Acquity I-Class (Milford, USA) UHPLC system with an Agilent Zorbax SB-C18 RRHD (Santa Clara, USA) reverse-phase column (2.1 × 50 mm, 1.8 µm). UHPLC–ESI (electrospray ionization) source mounted on a Xevo TQ-S Mass Spectrometer (Waters, Milford, USA) was used for CTC quantification. Mobile phase, solvent A (0.4% formic acid) and solvent B (acetonitrile) was optimized in a gradient elution as follows: 77.5% A (0-1.5 min), 10% A (1.51-2.5 min), 77.5% A (2.51-3 min) at acidic pH (2.7±0.5). Other parameters such as column temperature (30 ^{o}C), injection volume (1 µL) and flow rate (0.45 mL/min) were optimized for CTC quantification.

The mass spectrometer (MS/MS) was operated in positive ion mode and multiple reaction transitions (MRM) were used to monitor the CTC acquisition. The optimized MS/MS parameters in MRM with the highest intensity for CTC transitions including their precursor and production ions, cone voltage and collision energy are summarized in Supplementary Table 1. The production

ion 154 producing the highest intensity for CTC transition was used for quantitation and 444 transitions were used for confirmation of CTC. Other instrumental parameters used were as follows: spray voltage, 4.0 kV; collision gas, Argon at 0.15 ml/min; source temperature, 150 °C; cone gas flow, 150 L/h; desolvation temperature, gas flow, and pressure were 650°C, 1200 L/h, and 5.0 bar respectively. . The five-point calibration curve (5 µg/L to 200 µg/L) was prepared from a stock solution of 500 µg/L CTC in water. Positive electrospray ionization of mass spectrometric analysis was conducted with a mass scan range of m/z 50−500 to determine the CTC transformation products (Pulicharla et al., 2017).

2.3.3 Persulfate determination

Production of SO_4^{-*} was indirectly measured by determining the residual persulfate concentration during the experiment. A rapid iodometric method of persulfate anion determination developed by (Liang et al., 2008) was used to measure the residual persulfate left in the solution after 2h of experimental time. The reaction mixture containing, sodium persulfate stock solution/treated samples, $NaHCO_3$ and KI in Milli-Q water in glass vials were hand shaken and allowed to equilibrate for 15 min. Yellow iodine color formed from the reaction of PS with KI as shown in Eq. 11 was measured using a UV spectrophotometer at 352 nm. Experiments mean data and the standard deviation are presented in all figures.

$$S2O8^{2-} + 2I^{-} \rightarrow 2SO_4^{2-} + I_2 \qquad 12$$

2.3.4 Fe^{2+} and Fe^{3+} analysis

A spectrophotometric method was used to determine the Fe^{2+} and Fe^{3+} concentrations separately. 1,10-phenanthroline and sulfosalicylic acid indicator reagents were used to form complexes with Fe^{2+} (3:1, λ = 512 nm) and Fe^{3+} (1:1, λ = 490 nm) respectively, and the signal was measured in

acidic environment (pH ≈3) (Kozak et al., 2010) using UV/visible spectrophotometer (Varian Carey 50). A calibration curve of known $FeSO_4.7H_2O$ concentrations was used to calculate the iron concentration. These reagents are known to form stable complexes with respective iron ions in the acidic environment (Oktavia et al., 2008). Reagents concentration used in this study were sufficient to fully outcompete the CTC, resulting in negligible free Fe^{2+} and Fe^{3+} and CTC-Fe complexes.

2.4 Yeast Estrogen Screen (YES) assay

In order to screen the estrogenicity of the treated CTC, YES assay was carried out according to Routledge and Sumpter (1996) (Routledge and Sumpter, 1996) studies for PS/Fe^{2+} and PS/ZVI systems. Sterilization of all samples and standards (CTC and 17β-estradiol) were carried out prior to YES assay by serial dilutions with ethanol. Each concentration of standard and samples of 10 µL aliquots were transferred (triplicate) to a 96-well plate (Costar Brand, NY, USA) and waited,until completely dried. Aliquots (200 µL) of seeded assay medium containing the recombinant yeast (hER-transfected recombinant yeast) and the chlorophenol red-β-d-galactopyranoside (CPRG) chromogenic substrate were dispensed into each sample well. The plates were sealed with autoclave tape and mixed vigorously for 10 min in a shaker for 5min and incubated for 3 days at 32°C. The color of the assay medium was read after 3 days of incubation using a multireader microplate spectrophotometer (Epoch, BioTek, USA) at an absorbance of 540 nm.

2.5 Statistical analysis

Mean ± standard deviation (SD) was used to summarize the data in this study. Effect of PS/Fe^{2+} and PS/ZVI processes on the degradation of CTC data was statistically evaluated using analysis

of variance (ANOVA). Data from triplicates of CTC removal efficiency was expressed as the mean± standard error.

3. Results and discussion

3.1 CTC estimation

In the current work, solid phase extraction was used to break the CTC-Fe complex and to extract free CTC with small modifications in the reported method (Puicharla et al., 2014). EDTA concentration (1-10 mM) was optimized for complete release of CTC from CTC-Fe complexes and 3 mM EDTA was found to be optimum for 1 µM CTC. Mobile phase composed of 0.4% formic acid and ACN, was used in gradient elution system at pH 2.7±0.5 as mentioned in the section 2.3.1.2 showed 95% recovery of CTC. The calibration curve with five concentration levels (5–200 µg/L) showed good linearity with a correlation coefficient (R^2) of 0.995. Method validation parameters used in this study have been summarized in Supplementary Table 2.

It is worth underlining that less than 10% recovery of CTC was obtained in the presence of Fe^{2+} and ZVI using reported LC-MS/MS method (Daghrir et al., 2014). It has to be pointed out that this is not the drawback of this existing method, because the formed CTC-Fe complexes under current experimental conditions are not dissociated by the existing method (Wang et al., 2015) Direct injection of CTC solution after 30 min interaction with iron has given 77% recovery; where the overnight interaction has shown less than 10% CTC recovery (Supplementary Fig.S1). During the method development, it was also observed that basic pH 8.0 mobile phase (0.1% NH_4OH and ACN) is unable to give good recovery (15%) for CTC. Hence, small modifications wereperformed on the existing methods, such as EDTA concentration and mobile phase composition. High EDTA

concentration of 3 mM during solid phase extraction and0.4% formic acid in mobile phase resulted in 93–105% of CTC recovery.

3.2 Degradation of chlortetracycline by sulfate radicals

Fig. 2 shows the degradation efficiency of CTC by PS, $Fe^{2+,}$ and ZVI systems alone as positive controls. The removal efficiency was lower at low concentrations (100 µM) of PS, $Fe^{2+,}$ and ZVI and maximum removal of 54%, 44% and 42% CTC were observed at a highest concentration 5000 µM of respective controls. Even though PS is stable and did not produce any sulfate radicals at ambient temperature, it's high oxidation potential (E^0 = 2.01 V) was able to degrade CTC. In case of Fe^{2+}, it forms stable complexes with CTC and also undergoes autoxidation to Fe^{3+}. (Wang et al., 2015) studies reported the production of radicals such as O_2^{-*} and $OH^{\cdot}$ and also H_2O_2 during autoxidation of Fe^{2+}. These might beresponsible for the CTC degradation in the presence of Fe^{2+}. Similarly, increased Fe^{2+} concentration showed increased CTC degradation. On the other hand, CTC degradation by ZVI might have followed similar degradation pathways to Fe^{2+} as ZVI also generate soluble Fe^{2+} ions (Wang et al., 2015).

3.2.1 Optimization of PS/Fe^{2+} and PS/ZVI processes

PS and iron dose optimization studies were performed by taking the equal molar ratio (1:1) of PS/Fe^{2+} and PS/ZVI. Based on the stoichiometric Eq. 10, 48 times PS molar concentration is needed to completely mineralize one molar CTC. Taking this into consideration, five different molar concentrations ranging from 100-5000 µM of PS/Fe^{2+}/ZVI were studied. Fig. 3 represents the comparison of CTC removal efficiency by PS/Fe^{2+} and PS/ZVI processes at equal molar ratios. With the increasing molar concentration, increased removal CTC efficiency was seen in both PS/Fe^{2+} and PS/ZVI processes. Highest CTC removal of 87% and 94% was obtained in PS/Fe^{2+}

and PS/ZVI processes, respectively at the highest molar concentration 5000 µM. In control experiments, it was confirmed that PS alone can degrade 54% of CTC at its highest molar concentration (5000 µM). CTC degradation was increased to a large extent when Fe^{2+} and ZVI used as catalyst to activate the PS at room temperature (Fig. 3). Generation of SO_4^{-*} by activation of PS by Fe^{2+} and ZVI might be responsible for the higher degradation. And Fig. 3 clearly indicates that PS is activated by Fe^{2+} and ZVI with different efficiencies which resulted in different CTC removal percentages. The amount of sulfate radicals generation increased with increasing ratios and thus increased CTC removal. However, authors want to activate/utilize PS completely at low doses by increasing the catalyst (iron) concentration to generate SO_4^{-*} instead of using a high concentration of PS to remove CTC.

For iron dose optimization, 500 µM PS was taken as constant where 50% and 35% of PS was activated and 66% and 72% of CTC was degraded with an equal concentration of Fe^{2+} and ZVI, respectively (Fig. 3). Five different ratios of Fe^{2+} and ZVI with respect to PS were studied. Fig. 4 (A) shows the optimization study for iron concentration for maximum CTC removal. Two times the PS concentration of iron (1:2) showed 76%±3.4 and 93%±2.9 CTC removal in both PS/Fe^{2+} and PS/ZVI processes, respectively. Fig. 4 (B) represents the used PS for the formation of sulfate radicals. In PS/Fe^{2+} and PS/ZVI processes at 1:2 molar ratio, 91%±2.3 and 53%±1.8 of PS has been activated to remove CTC, respectively. Even though PS consumption is high (91%) in PS/Fe^{2+} process at 1:2 molar ratio, high CTC removal was observed in PS/ZVI process at 53% PS activation. Rapid PS activation, high availability of sulfate radicals and Fe^{2+} ions in PS/Fe^{2+} process were not aiding in efficient degradation of CTC.

In case of PS/ZVI system, the release of Fe^{2+} from Fe^0 and further oxidation of Fe^{2+} to Fe^{3+} were the two principal reactions involved in the activation of PS. This continuous and slow release of

Fe^{2+} ions from heterogeneous phase (Fe^0) might activate PS slowly and generate sulfate radicals. Meanwhile, in a homogeneous system, absolute availability of Fe^{2+} (soluble) was desired to activate all PS molecules to generate sulfate radicals at a time. Many studies have explained the high efficiency of controlled generation of sulfate radicals by ZVI catalyst in the degradation of emerging pollutants (Rodriguez et al., 2014; Rodriguez et al., 2017). At 1:2 (PS/Fe^{2+}) ratio, above 90% of PS was activated, but CTC removal was increased by only 10% (77%) compared to 1:1 molar ratio where 37% of PS was consumed. Increased activation of PS did not show corresponding increase in CTC degradation. This is due to the fact that higher generation of SO_4^{-*} might act as a scavenger itself as given in Eq. 5 (Xu and Li, 2010) and also the higher Fe^{2+} concentration can also scavenge SO_4^{-*} as given in Eq. 4 (McElroy and Waygood, 1990). Many studies have reported that PS:Fe^{2+} molar ratio over 1:1 was not efficient in oxidizing organic contaminants as generated SO_4^{-*} are getting scavenged by other side reactions as Eq. 4, 5, and 6 (Brandt and Van Eldik, 1995; Rastogi et al., 2009). In contrast, only half activated PS (53%) results in 93% CTC removal by ZVI at 1:2 (PS/ZVI). Therefore, activation of PS by the heterogeneous source of iron is more efficient compared the homogenous source of iron under identical conditions. These results indicated that the removal efficiency of CTC could be enhanced by ZVI instead of Fe^{2+} addition. The estimation of Fe^{2+} concentration after 2h reaction evidenced that slow activation of PS is effective in CTC degradation.

Above 80% of total Fe^{2+} was oxidized to Fe^{3+} in case of PS/Fe^{2+} (1:2) wherein PS/ZVI reaction, 95% of dissolved Fe^{2+} after 2h from ZVI (25-30%) was oxidized to Fe^{3+}. Low Fe^{3+} in PS/ZVI (1:2) was seen at the end (2h) compared to PS/Fe^{2+} reaction which is due to less available Fe^{2+} concentration undergone oxidation to Fe^{3+} (data is not presented). Additional kinetic studies on Fe^{2+} and Fe^{3+} formation in PS/ZVI process are necessary to evaluate the sulfate radicals generation

and Fe^{2+} oxidation rates. These studies might be helpful to find the optimum PS dose and rate of Fe^{2+} regeneration.

3.2.2 Effect of pH on CTC degradation

Optimum conditions of PS/Fe^{2+} and PS/ZVI processes (1:2) where highest CTC removal was observed was considered to investigate the pH effect on CTC degradation. Five different pH values including 3.0, 4.5, 6.0, 8.0 and 10.0 were studied and pH adjustment was done using NaOH or HCl. As seen in Fig. 5, CTC removal was slightly decreased with the increasing pH. Final pH after the 2h reaction was recorded as follows 2.68, 2.66, 2.8, 3.1 and 3.5 for respective studied initial pHs. As seen in the Eq. 10, production of sulfuric acid during the reaction could be the reason for the drop of pH during the 2h reaction time. CTC removal efficiency was nearly the same until pH 8 but 15% decrease in removal was seen at pH 10. As reported, SO_4^{-*} can be produced at a wide range of pH (2-8) but the decreased removal at higher pH can be due to scavenging of SO_4^{-*} by $OH^{\bullet}$ (Eq. 6) (Liang et al., 2007) and decreased oxidation potential of OH^{*} radicals with increasing pH.

The final removal efficiencies were 75%, 76%, 74%, 69% and 62% for Fe^{2+} and 94%, 92%, 92%, 88% and 78% for ZVI at pH 3.0, 4.5, 6.0, 8.0 and 10.0, respectively as shown in Fig. 5. In this study, pH is not maintained by adding any buffering solution, only initial pH effect was investigated to avoid unnecessary interactions among buffering reagents, SO_4^{-*} radicals, and CTC. From these results, it is very clear that the CTC degradation efficiency is not affected by the initial pH in both systems from pH 3.0–8.0. These results of pH effect is in agreement with the previous studies of (Hou et al., 2012) where slight decrease in tetracycline degradation from 89 to 85% was

reported with increasing pH 3 to 9. Nearly similar final pH value at the end of all experiments stated the similar degradation efficiencies despite the different initial pH values.

3.3 Identification of degradation products and proposed pathways

Treated solution of CTC in PS/Fe^{2+} and PS/ZVI processes at 1:2 molar ratio were used to identify the degradation products by LC-MS/MS. According to the MS spectrometric results, the possible mechanisms through which sulfate radicals degraded CTC under PS/Fe^{2+} and PS/ZVI processes is proposed in Fig. 6. The chromatographic peaks of the respective reported by-products are given in Supplementary figure S2. The intermediates formed during the degradation process were identified and reported for the first time by sulfate radicals in this study. Both processes have shown similar transformation products (TPs), such as m/z 303 and 184 with highest intensities compared to parent compound. Both processes attacked CTC in similar fashion by demethylation, deamination dehydroxylation reactions, but the formed end degradation products were dissimilar. This might be due to higher efficiency of PS/ZVI process which might degrade CTC to lower mass TPs compared to PS/Fe^{2+} system. Formation of lower mass and dechlorinated TPs in this study showed that sulfate radicals are generally efficient in degrading organic contaminants having chlorine in their structure.

3.4 Estrogenicity assessment of PS/Fe^{2+} and PS/ZVI treated CTC samples

Estrogenicity test was performed mainly to determine the estrogenic capacity of the treated solution containing degradation by-products, residual CTC and PS concentration. CTC at 1µM did not show any estrogenic effect and this test revealed the toxicity of formed by-products after degradation. Estrogen activity of experiments (500:1000 µM (1:2); PS/Fe^{2+} and PS/ZVI processes) which showed highest CTC removal was carried out by YES assay. The response of estrogenic

activity of standard 17β-estradiol (5 ng/L to 50mg/L) concentrations showed absorbance within 1 to 1.2 range after three days incubation. Before incubation, all samples including blank, standard and samples showed yellow color and depending on the estrogen activity, the samples turned into red. CTC spiked in Milli-Q water before and after treatment with PS/Fe^{2+} and PS/ZVI processes had shown no estrogenic activity (no color change) compared to tested standard 17β-estradiol standard samples. Assay medium treated with standard 17β-estradiol only showed red color and remaining samples including blank (alcohol), spiked and treated CTC samples did not show any color change to red (remained in yellow color). The different TPs of both PS/Fe^{2+} and PS/ZVI processes (Fig.6) which are not completely similar did not show any estrogenicity. Controls having Fe^{2+}, ZVI and PS samples also did not shown any estrogenic activity. Hence, the used PS (500 µM) and iron concentrations (1000 µM) in this study were not toxic. As per author's knowledge, this is the first time reporting the estrogenic activity of PS and iron concentrations and also the CTC degradation by SO_4^{-*}. Hence, SO_4^{-*} oxidation can be considered as a safe and efficient technique in degrading CTC.

4. Conclusion

Free CTC after complexation with iron was measured with 95% recovery in currently developed UHPLC method. SPE with optimized EDTA (3mM) is necessary to break the CTC-Fe complex before injecting the sample into UHPLC to estimate CTC. In the present study, CTC was successfully degraded by environmental friendly SO_4^{-*} based AOP. It was found that heterogeneous activation (ZVI) is more efficient than homogeneous activation (Fe^{2+}) of PS to degrade CTC. PS/Fe^{2+} and PS/ZVI processes showed 76% and 94% degradation of 1 µM CTC at 1:2 molar ratio as optimum in 2h at 500 µM PS and 1000 µM iron. All Fe^{2+} ions in the case of homogeneous reaction activated above 90% PS to produce SO_4^{-*} which seemed to be not efficient

in degrading CTC due to scavenging of sulfate radicals by itself and also by excess Fe^{2+} ions. Whereas in heterogeneous reactions, slow generation and regeneration of Fe^{2+} ions might be helping in removal of CTC above 90%. Hence, heterogeneous activation by iron catalyst which is not in the same dissolved phase as PS demonstrated superior performance in CTC removal than homogeneous activation under similar conditions. Further, the formed dechlorinated end products stated that SO_4^{-*} is the most effective technique in degrading CTC to non-toxic by-products.

Acknowledgment

The authors are sincerely thankful to the Natural Sciences and Engineering Research Council of Canada (Discovery Grant 355254 and Strategic Grant), and Ministère des Relations Internationales du Québec (coopération Québec-Catalanya 2012–2014, 01.801-23525) for financial support. Authors are also thankful to "merit scholarship program for foreign students" (FQRNT) for financial assistance to Rama Pulicharla. Thanks to Prof. Viviane Yargeau for providing YES test yeast strain from McGill University to perform estrogenicity study.

References

An, J., Chen, H., Wei, S., Gu, J., 2015. Antibiotic contamination in animal manure, soil, and sewage sludge in Shenyang, northeast China. Environmental Earth Sciences 74, 5077-5086.

Anipsitakis, G.P., Dionysiou, D.D., 2004. Radical generation by the interaction of transition metals with common oxidants. Environmental science & technology 38, 3705-3712.

Brandt, C., Van Eldik, R., 1995. Transition metal-catalyzed oxidation of sulfur (IV) oxides. Atmospheric-relevant processes and mechanisms. Chemical Reviews 95, 119-190.

Daghrir, R., Drogui, P., Delegan, N., El Khakani, M.A., 2013. Electrochemical degradation of chlortetracycline using N-doped Ti/TiO 2 photoanode under sunlight irradiations. Water research 47, 6801-6810.

Daghrir, R., Drogui, P., Delegan, N., El Khakani, M.A., 2014. Removal of chlortetracycline from spiked municipal wastewater using a photoelectrocatalytic process operated under sunlight irradiations. Science of The Total Environment 466–467, 300-305.

Daghrir, R., Drogui, P., Ka, I., El Khakani, M.A., 2012. Photoelectrocatalytic degradation of chlortetracycline using Ti/TiO 2 nanostructured electrodes deposited by means of a pulsed laser deposition process. Journal of hazardous materials 199, 15-24.

Deng, J., Shao, Y., Gao, N., Deng, Y., Tan, C., Zhou, S., 2014. Zero-valent iron/persulfate (Fe0/PS) oxidation acetaminophen in water. International Journal of Environmental Science and Technology 11, 881-890.

Gao, Y., Zhang, Z., Li, S., Liu, J., Yao, L., Li, Y., Zhang, H., 2016. Insights into the mechanism of heterogeneous activation of persulfate with a clay/iron-based catalyst under visible LED light irradiation. Applied Catalysis B: Environmental 185, 22-30.

Gogate, P.R., Pandit, A.B., 2004. A review of imperative technologies for wastewater treatment I: oxidation technologies at ambient conditions. Advances in Environmental Research 8, 501-551.

Guo, R., Chen, J., 2012. Phytoplankton toxicity of the antibiotic chlortetracycline and its UV light degradation products. Chemosphere 87, 1254-1259.

Hammad Khan, M., Jung, H.-S., Lee, W., Jung, J.-Y., 2013. Chlortetracycline degradation by photocatalytic ozonation in the aqueous phase: mineralization and the effects on biodegradability. Environmental technology 34, 495-502.

Hou, L., Zhang, H., Xue, X., 2012. Ultrasound enhanced heterogeneous activation of peroxydisulfate by magnetite catalyst for the degradation of tetracycline in water. Separation and Purification Technology 84, 147-152.

Karthikeyan, K.G., Meyer, M.T., 2006. Occurrence of antibiotics in wastewater treatment facilities in Wisconsin, USA. Science of The Total Environment 361, 196-207.

Kim, T.-H., Kim, S.D., Kim, H.Y., Lim, S.J., Lee, M., Yu, S., 2012. Degradation and toxicity assessment of sulfamethoxazole and chlortetracycline using electron beam, ozone and UV. Journal of hazardous materials 227, 237-242.

Kozak, J., Gutowski, J., Kozak, M., Wieczorek, M., Kościelniak, P., 2010. New method for simultaneous determination of Fe (II) and Fe (III) in water using flow injection technique. Analytica chimica acta 668, 8-12.

Lau, T.K., Chu, W., Graham, N.J., 2007. The aqueous degradation of butylated hydroxyanisole by UV/S2O82-: study of reaction mechanisms via dimerization and mineralization. Environmental science & technology 41, 613-619.

Lee, Y., von Gunten, U., 2010. Oxidative transformation of micropollutants during municipal wastewater treatment: comparison of kinetic aspects of selective (chlorine, chlorine dioxide, ferrate VI, and ozone) and non-selective oxidants (hydroxyl radical). Water Research 44, 555-566.

Liang, C., Bruell, C.J., Marley, M.C., Sperry, K.L., 2004. Persulfate oxidation for in situ remediation of TCE. I. Activated by ferrous ion with and without a persulfate–thiosulfate redox couple. Chemosphere 55, 1213-1223.

Liang, C., Guo, Y.-y., 2010. Mass transfer and chemical oxidation of naphthalene particles with zerovalent iron activated persulfate. Environmental science & technology 44, 8203-8208.

Liang, C., Huang, C.-F., Mohanty, N., Kurakalva, R.M., 2008. A rapid spectrophotometric determination of persulfate anion in ISCO. Chemosphere 73, 1540-1543.

Liang, C., Liang, C.-P., Chen, C.-C., 2009. pH dependence of persulfate activation by EDTA/Fe (III) for degradation of trichloroethylene. Journal of contaminant hydrology 106, 173-182.

Liang, C., Wang, Z.-S., Bruell, C.J., 2007. Influence of pH on persulfate oxidation of TCE at ambient temperatures. Chemosphere 66, 106-113.

Lin, Y.-T., Liang, C., Yu, C.-W., 2016. Trichloroethylene degradation by various forms of iron activated persulfate oxidation with or without the assistance of ascorbic acid. Industrial & Engineering Chemistry Research 55, 2302-2308.

Lindsey, M.E., Meyer, M., Thurman, E., 2001. Analysis of trace levels of sulfonamide and tetracycline antimicrobials in groundwater and surface water using solid-phase extraction and liquid chromatography/mass spectrometry. Analytical chemistry 73, 4640-4646.

Luo, Q., 2014. Oxidative treatment of aqueous monochlorobenzene with thermally-activated persulfate. Frontiers of Environmental Science & Engineering 8, 188-194.

McElroy, W., Waygood, S., 1990. Kinetics of the reactions of the SO–4 radical with SO–4, S2O2–8, H2O and Fe2+. Journal of the Chemical Society, Faraday Transactions 86, 2557-2564.

Mecha, A.C., Onyango, M.S., Ochieng, A., Fourie, C.J.S., Momba, M.N.B., 2016. Synergistic effect of UV–vis and solar photocatalytic ozonation on the degradation of phenol in municipal wastewater: A comparative study. Journal of Catalysis 341, 116-125.

Miao, X.-S., Bishay, F., Chen, M., Metcalfe, C.D., 2004. Occurrence of antimicrobials in the final effluents of wastewater treatment plants in Canada. Environmental science & technology 38, 3533-3541.

Michael-Kordatou, I., Andreou, R., Iacovou, M., Frontistis, Z., Hapeshi, E., Michael, C., Fatta-Kassinos, D., 2017. On the capacity of ozonation to remove antimicrobial compounds, resistant bacteria and toxicity from urban wastewater effluents. Journal of Hazardous Materials 323, Part A, 414-425.

Miralles-Cuevas, S., Oller, I., Pérez, J.A.S., Malato, S., 2014. Removal of pharmaceuticals from MWTP effluent by nanofiltration and solar photo-Fenton using two different iron complexes at neutral pH. Water Research 64, 23-31.

Monteagudo, J., Durán, A., González, R., Expósito, A., 2015. In situ chemical oxidation of carbamazepine solutions using persulfate simultaneously activated by heat energy, UV light, Fe 2+ ions, and H 2 O 2. Applied Catalysis B: Environmental 176, 120-129.

Munoz, M., Garcia-Muñoz, P., Pliego, G., Pedro, Z.M.d., Zazo, J.A., Casas, J.A., Rodriguez, J.J., 2016. Application of intensified Fenton oxidation to the treatment of hospital wastewater: Kinetics, ecotoxicity and disinfection. Journal of Environmental Chemical Engineering 4, 4107-4112.

Oh, S.-Y., Kim, H.-W., Park, J.-M., Park, H.-S., Yoon, C., 2009. Oxidation of polyvinyl alcohol by persulfate activated with heat, Fe 2+, and zero-valent iron. Journal of hazardous materials 168, 346-351.

Oktavia, B., Lim, L.W., Takeuchi, T., 2008. Simultaneous determination of Fe (III) and Fe (II) ions via complexation with salicylic acid and 1, 10-phenanthroline in microcolumn ion chromatography. Analytical Sciences 24, 1487-1492.

Paul, T., Miller, P.L., Strathmann, T.J., 2007. Visible-light-mediated TiO2 photocatalysis of fluoroquinolone antibacterial agents. Environmental science & technology 41, 4720-4727.

Puicharla, R., Mohapatra, D., Brar, S., Drogui, P., Auger, S., Surampalli, R., 2014. A persistent antibiotic partitioning and co-relation with metals in wastewater treatment plant—chlortetracycline. Journal of Environmental Chemical Engineering 2, 1596-1603.

Pulicharla, R., Brar, S.K., Rouissi, T., Auger, S., Drogui, P., Verma, M., Surampalli, R.Y., 2017. Degradation of chlortetracycline in wastewater sludge by ultrasonication, Fenton oxidation, and ferro-sonication. Ultrasonics Sonochemistry 34, 332-342.

Pulicharla, R., Das, R.K., Brar, S.K., Drogui, P., Sarma, S.J., Verma, M., Surampalli, R.Y., Valero, J.R., 2015. Toxicity of chlortetracycline and its metal complexes to model microorganisms in wastewater sludge. Science of the Total Environment 532, 669-675.

Qin, D., Lu, W., Wang, X., Li, N., Chen, X., Zhu, Z., Chen, W., 2016. Graphitic Carbon Nitride from Burial to Re-emergence on Polyethylene Terephthalate Nanofibers as an Easily Recycled Photocatalyst for Degrading Antibiotics under Solar Irradiation. ACS Applied Materials & Interfaces 8, 25962-25970.

Rastogi, A., Al-Abed, S.R., Dionysiou, D.D., 2009. Sulfate radical-based ferrous–peroxymonosulfate oxidative system for PCBs degradation in aqueous and sediment systems. Applied Catalysis B: Environmental 85, 171-179.

Rodriguez, S., Santos, A., Romero, A., 2017. Oxidation of priority and emerging pollutants with persulfate activated by iron: Effect of iron valence and particle size. Chemical Engineering Journal 318, 197-205.

Rodriguez, S., Vasquez, L., Romero, A., Santos, A., 2014. Dye oxidation in aqueous phase by using zero-valent iron as persulfate activator: kinetic model and effect of particle size. Industrial & Engineering Chemistry Research 53, 12288-12294.

Romero, A., Santos, A., Vicente, F., González, C., 2010. Diuron abatement using activated persulphate: effect of pH, Fe (II) and oxidant dosage. Chemical Engineering Journal 162, 257-265.

498 Routledge, E.J., Sumpter, J.P., 1996. Estrogenic activity of surfactants and some of their degradation
499 products assessed using a recombinant yeast screen. Environmental toxicology and chemistry 15, 241-
500 248.
501 Triszcz, J.M., Porta, A., Einschlag, F.S.G., 2009. Effect of operating conditions on iron corrosion rates in
502 zero-valent iron systems for arsenic removal. Chemical Engineering Journal 150, 431-439.
503 Vicente, F., Santos, A., Romero, A., Rodriguez, S., 2011. Kinetic study of diuron oxidation and
504 mineralization by persulphate: effects of temperature, oxidant concentration and iron dosage method.
505 Chemical engineering journal 170, 127-135.
506 Wang, H., Yao, H., Sun, P., Li, D., Huang, C.-H., 2015. Transformation of tetracycline antibiotics and Fe (II)
507 and Fe (III) species induced by their complexation. Environmental science & technology 50, 145-153.
508 Wilmarth, W., Haim, A., Edwards, J., 1962. Mechanisms of Oxidation by Peroxydisulfate Ion in Peroxide
509 Reaction Mechanisms. Wiley-Interscience, New York.
510 Xu, X.-R., Li, X.-Z., 2010. Degradation of azo dye Orange G in aqueous solutions by persulfate with ferrous
511 ion. Separation and purification technology 72, 105-111.
512 Zhou, L., Zheng, W., Ji, Y., Zhang, J., Zeng, C., Zhang, Y., Wang, Q., Yang, X., 2013. Ferrous-activated
513 persulfate oxidation of arsenic (III) and diuron in aquatic system. Journal of hazardous materials 263, 422-
514 430.

515

516

517

518

519

520

521

522

523

524

525

Figure captions:

Figure 1. Chlortetracycline structure showing the iron binding site.

Figure 2. Degradation of chlortetracycline with persulfate, Fe^{2+} and zero valent iron (ZVI) individually (CTC= 1 µM, treatment time=2h)

Figure 3. Comparison of chlortetracycline (CTC) degradation efficiency of Fe^{2+} and zero-valent iron (Fe^{0}) by activating persulfate (PS) at equal molar concentrations (CTC= 1 µM, treatment time=2h, pH=3-4)

Figure 4. Optimization of Fe^{2+} and zero valent iron (ZVI) concentration: A) degradation of chlortetracycline (CTC); and B) reduction of persulfate (persulfate 500 µM and CTC= 1 µM, treatment time=2h, pH=3-4).

Figure 5. Effect of pH on the degradation of chlortetracycline (CTC) (CTC = 1 µM; PS:Fe^{2+} and PS:ZVI; 1:2 = 500:1000 µM, treatment tine=2h).

Figure 6. Transformation products and proposed degradation pathways of CTC: A) PS/Fe^{2+} process; and B) PS/ZVI process

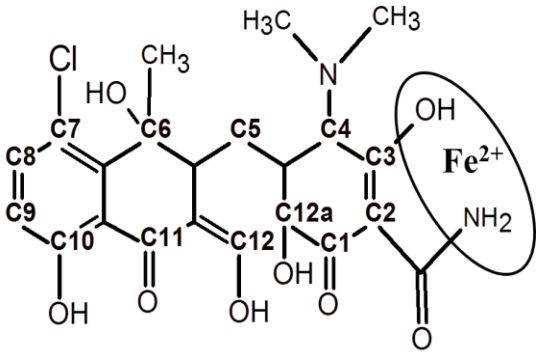

Figure 1. Chlortetracycline structure showing the iron binding site.

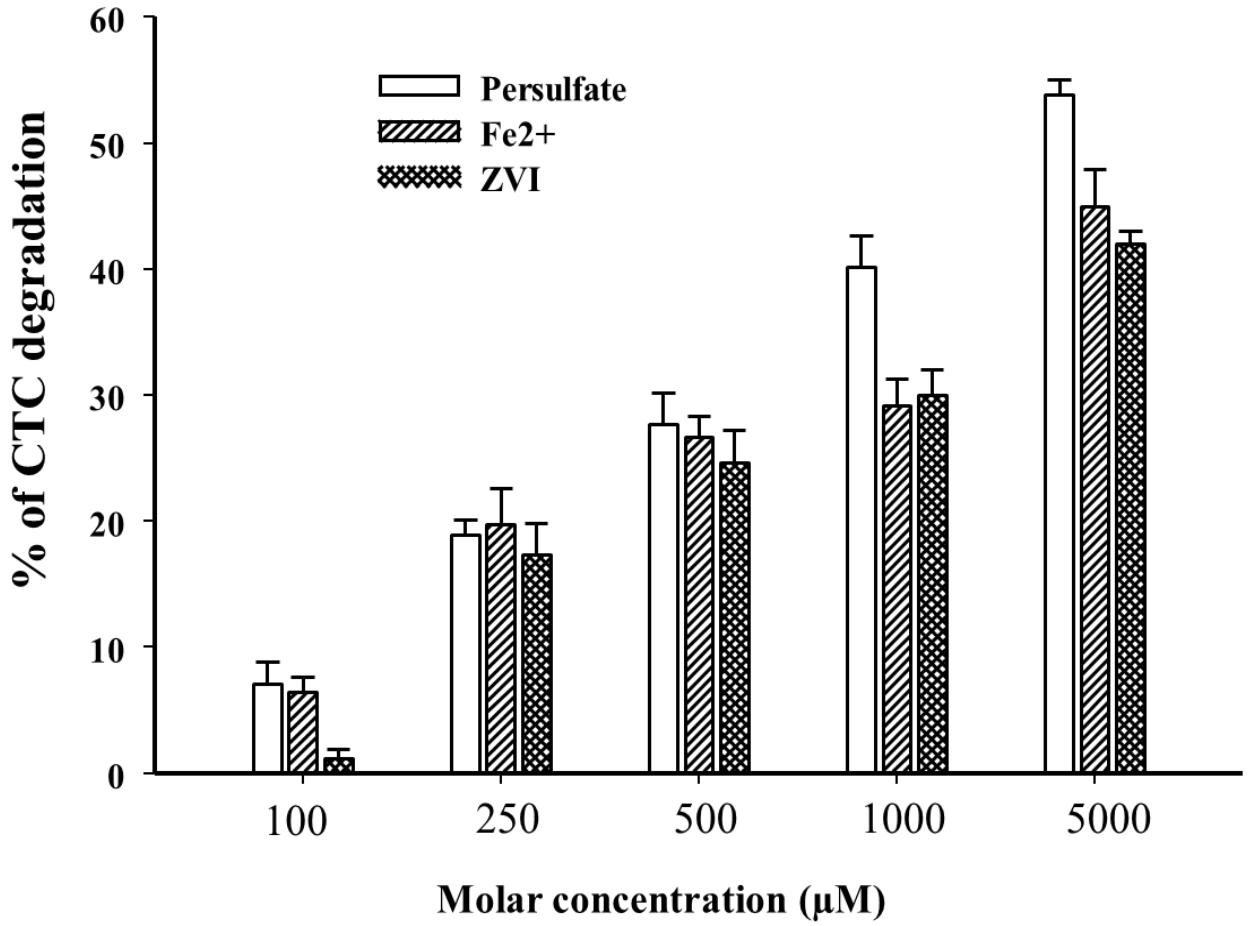

Figure 2. Degradation of chlortetracycline with persulfate, Fe^{2+} and zero valent iron (ZVI) individually (CTC= 1 µM, treatment time=2h)

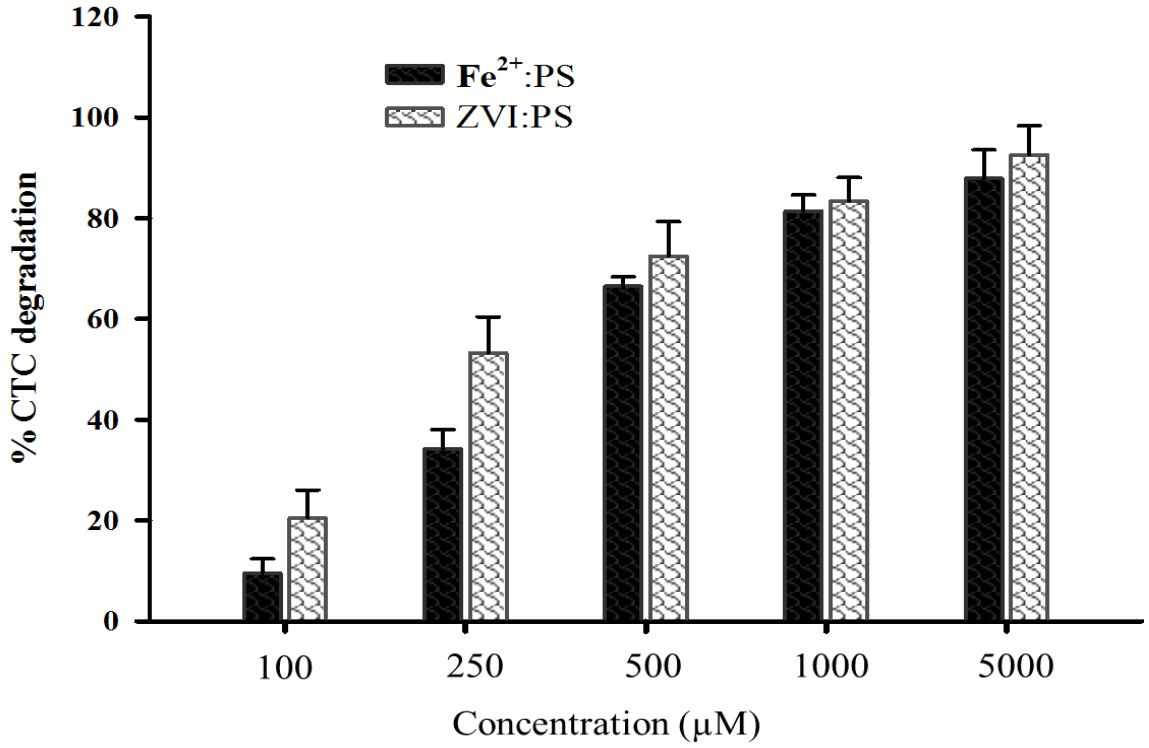

Figure 3. Comparison of chlortetracycline (CTC) degradation efficiency of Fe^{2+} and zero-valent iron (Fe^{0}) by activating persulfate (PS) at equal molar concentrations (CTC= 1 μM, treatment time=2h, pH=3-4)

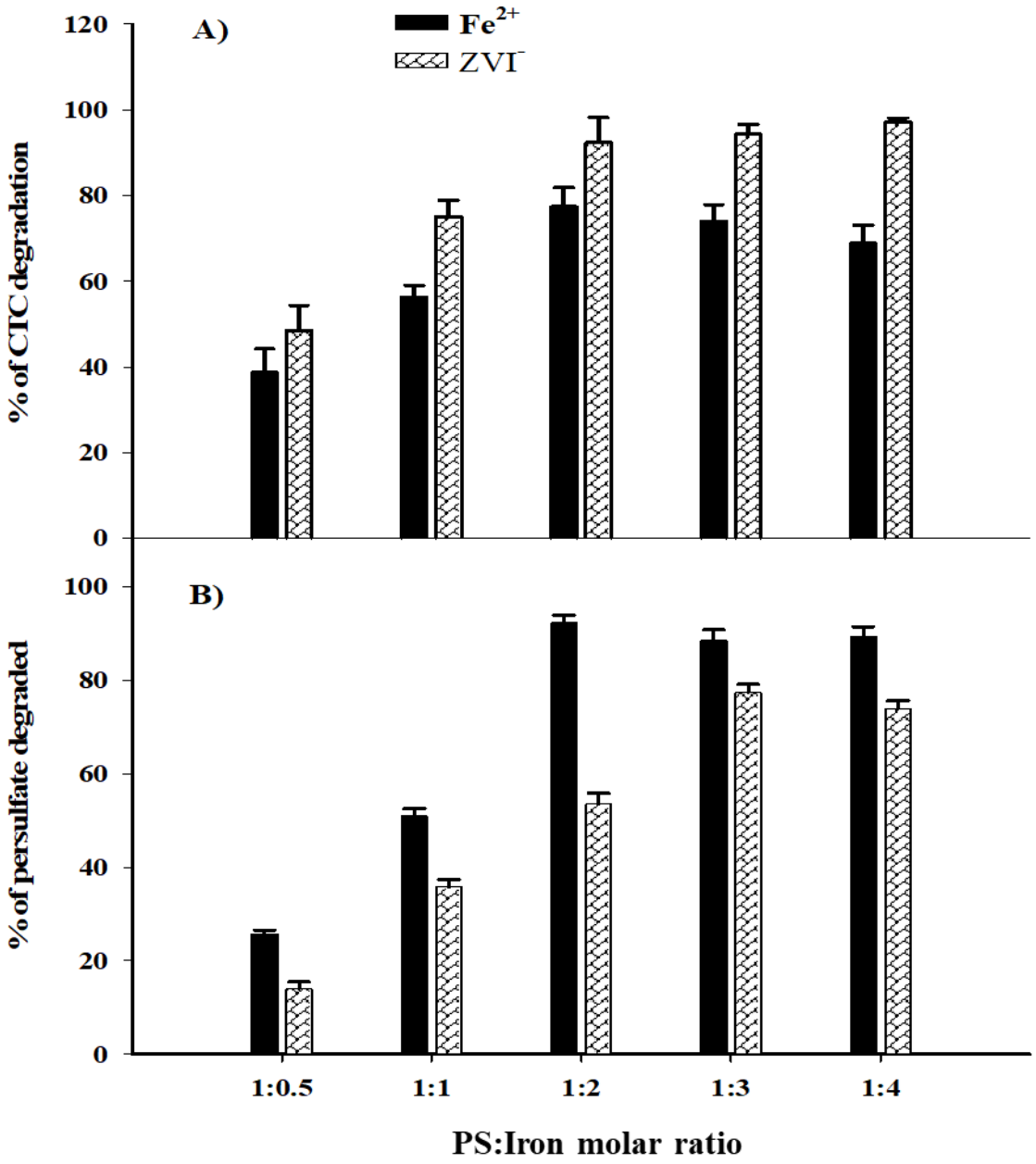

Figure 4. Optimization of Fe^{2+} and zero valent iron (ZVI) concentration: A) degradation of chlortetracycline (CTC); and B) reduction of persulfate (persulfate (PS) 500 µM and CTC= 1 µM, treatment time=2h, pH=3-4).

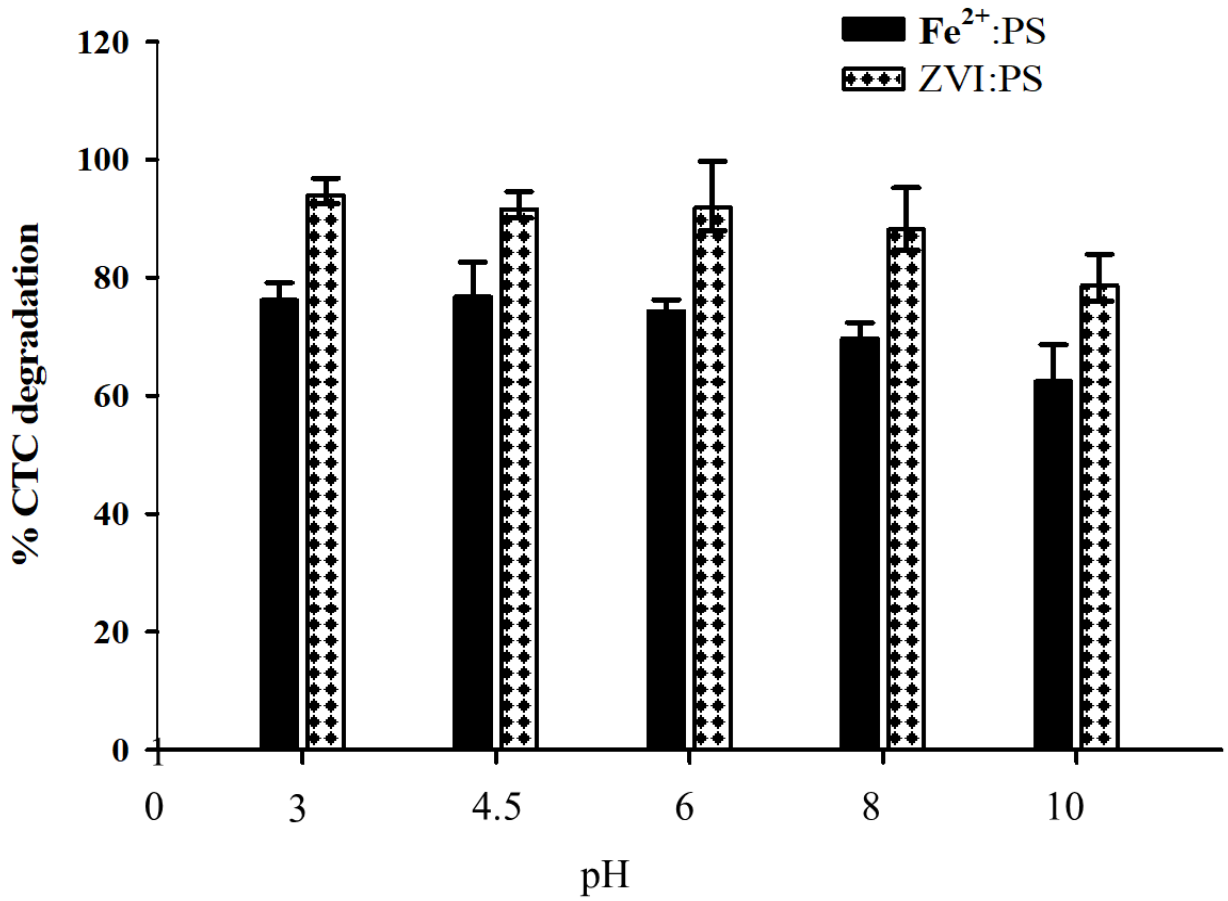

Figure 5. Effect of pH on the degradation of chlortetracycline (CTC) (CTC = 1 μM; PS:Fe^{2+} and PS:ZVI; 1:2 = 500:1000 μM, treatment tine=2h).

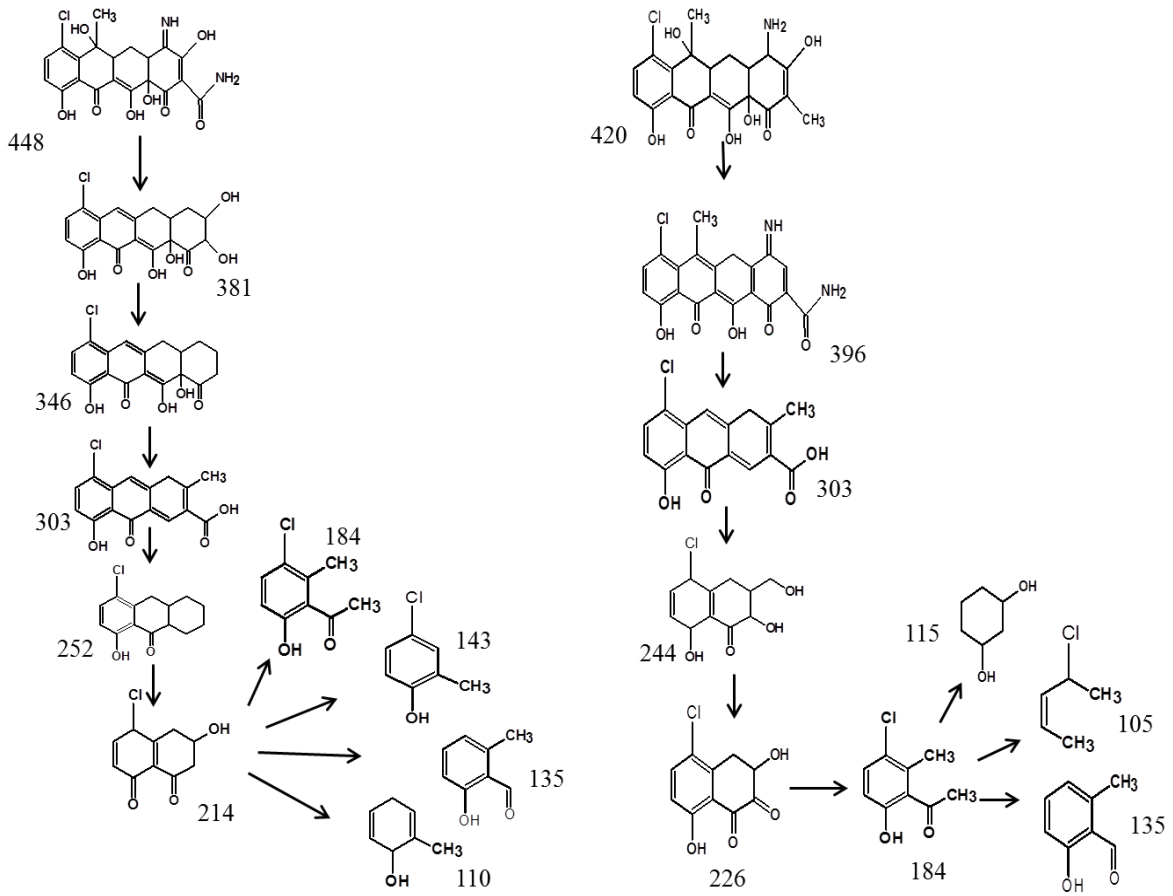

Figure 6. Transformation products and proposed degradation pathways of CTC: A) PS/Fe^{2+} process (PS:Fe^{2+} ; 1:2 = 500:1000 µM); and B) PS/ZVI process (PS:ZVI; 1:2 = 500:1000 µM); (CTC = 1 µM, treatment tine=2h)